Star Clusters: From the Milky Way to the Early Universe
Proceedings IAU Symposium No. 351, 2019
A. Bragaglia, M. Davies, A. Sills & E. Vesperini, eds.

doi:10.1017/S1743921319006616

The chemical feature of Miras in 47 Tuc based on the WINERED spectra

Y. Wang[1], V. D'Orazi[2,3], N. Matsunaga[4,5] and G. Bono[6,7]

[1]Key Laboratory of Optical Astronomy, National Astronomical Observatories, Chinese Academy of Sciences, Beijing, China
email: ywang@nao.cas.cn

[2]INAF Osservatorio Astronomico di Padova, Padova, Italy

[3]Monash Centre for Astrophysics, School of Physics and Astronomy, Monash University, Melbourne, Australia

[4]Department of Astronomy, The University of Tokyo, Tokyo, Japan

[5]Laboratory of infrared High-resolution spectroscopy (LiH), Koyama Astronomical Observatory, Kyoto-Sangyo University, Motoyama, Kamigamo, Kita-ku, Kyoto, Japan

[6]University of Roma Tor Vergata, Roma, Italy

[7]INAF Osservatorio Astronomico di Roma, Monte Porzio Catone RM, Italy

Abstract. Variable stars are good stellar tracers. Among various variables, Miras have long periods and are at the evolutionary phase of asymptotic giant branch. Their low effective temperatures lead to a difficulty to determine their chemical composition that since plenty of molecular bands exist in their spectra which even blocks the identifition of metallic lines. However, molecular features are less common in near-infrared (NIR) compared with other wavelength ranges. Here we take advantage of the high-resolution (R $\sim$ 28, 000) spectra obtained with WINERED, which is a NIR spectrograph covering the wavelength range of 0.91−1.35 μm, to analyze and determine the chemical abundances of three Miras in the Galactic globular cluster 47 Tuc (NGC 104). Steps of data reduction and analysis, as well as part of the preliminary results, are briefly shown.

Keywords. stars: variables: other, infrared: stars, stars: abundances, globular clusters: individual (NGC 104)

1. Introduction

It is well known that variable stars are good stellar tracers considering the advantage that robust individual distances, ages and reddening can be derived for each of them, allowing us to determine their spatial variations in a three-dimensional space. Miras are long-period variables at the evolutionary phase of asymptotic giant branch. However, the complex dynamical nature of their extended atmospheres makes it hard to measure chemical abundances for Miras (Lebzelter *et al.* 2014). Moreover, with the low effective temperatures, around 3000 K or lower, plenty of molecular bands exist in their spectra which makes it even difficult to identify the metallic lines. In this context, WINERED, a near-infrared (NIR) high-resolution (R $\sim$ 28,000, WIDE mode) spectrograph covering the wavelength range of 0.91−1.35 μm, provides a good opportunity to study the chemical abundances of Miras, because molecular features are less common in NIR compared with other wavelength ranges and certain metallic lines can be easily identified. Miras in clusters also have the advantage that the clusters often have been well studied, so that some priori information about the chemical composition, the environment and the evolutionary channel can be obtained for the Miras. In this work, we use the spectra

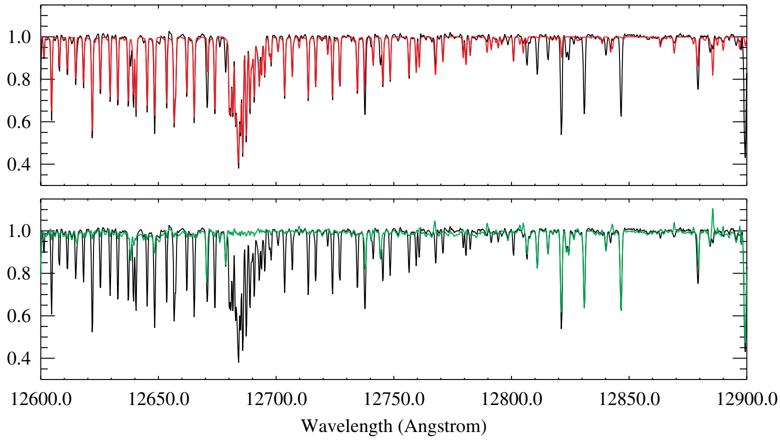

Figure 1. An example of the telluric correction, where the original spectra of V11 are in black in the two panels, and the modelled telluric spectrum (red) and the corrected spectrum (green) are shown in the top and bottom panel, respectively.

collected with WINERED to determine and analyze the chemical abundances of iron, α-elements and some other elements for three Miras in the Galactic globular cluster 47 Tuc (NGC 104).

2. Observation and Data Reduction

We have three Miras, V1, V3 and V11, selected from the Galactic globular cluster 47 Tuc in our sample (see Table 1). They were observed with the WIDE mode (R $\sim$ 28,000) of WINERED, a PI instrument attached to the 3.58-m New Technology Telescope (NTT) at La Silla observatory, ESO, Chile.

The data reduction was performed using the automated pipeline developed by the WINERED team (e.g. Taniguchi *et al.* 2018). Before we started the abundance analysis, the absorption features caused by the atmosphere of the Earth, i.e. the telluric lines, must be removed from the spectra. Here the synthetic sky modeller TelFit by Gullikson *et al.* (2014) was used to compute the telluric spectra for individual target spectra. Figure 1 shows a comparison among the original spectrum of V11, the modelled telluric spectrum and the spectrum after the telluric correction.

3. Stellar Atmospheric Parameters

By cross-matching the observed spectra with the synthesized model spectrum in the 11,700 $-$ 13,200 Å region, we determined the radial velocity (RV) for the Miras. After the barycentric correction, their RVs are $6.38\,km\,s^{-1}$ (V1), $-19.76\,km\,s^{-1}$ (V3) and $-23.36\,km\,s^{-1}$ (V11), respectively. Since the sample stars are variables, their RVs vary with time. The RV values we derived are consistent with those by Lebzelter *et al.* (2005).

The periods of the three Miras were determined using the V-band ASAS-SN data (Shappee *et al.* 2014; Kochanek *et al.* 2017) of the most recent 1000 days, although that of V11 is not so clear. The infrared magnitudes were estimated using the photometry obtained with the 1.4-m Infrared Survey Facility (IRSF). The phased light curves in V and Ks bands are shown in Figure 2. In Table 1 we list the derived magnitudes and periods.

The stellar effective temperature ($T_{\rm eff}$) was determined with the J-Ks color using the calibration by Alonso *et al.* (1999). Considering the reddening value from Bono *et al.* (2008) of E(B-V) = 0.04, which corresponds to E(J-Ks) = 0.02 based on the extinction

https://doi.org/10.1017/S1743921319006616 Published online by Cambridge University Press

Table 1. The coordinates, magnitudes and periods of the Miras.

ID	RA (J2000)	Dec (J2000)	V	Ks	J-Ks	V-Ks	Period (days)
V1	00:24:12.7	-72:06:40	14.40*	6.30	1.15	8.10*	213.2
V3	00:25:16.0	-72:03:55	12.80	6.50	1.10	6.30	192.4
V11	00:25:09.1	-72:02:16	11.80	6.60	1.10	5.20	138.6

Note: According to the light curve, we doubt the photometry of V1 at the faint phase derived from ASAS-SN data are polluted, and we use '*' to mark the questionable V mag and V-Ks.

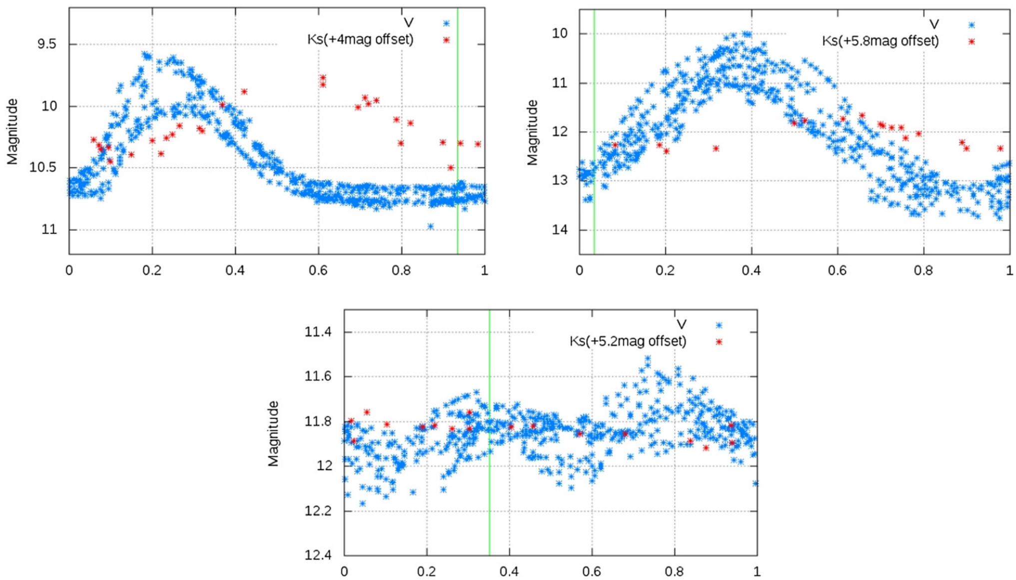

Figure 2. Phased light curves of the Miras sample in V (blue) and Ks (red) bands. The vertical green line shows the phase where the observation was done.

law of Cardelli *et al.* (1989), $T_{\rm eff} = 3600\,{\rm K}$ was derived for both V3 and V11, while V1 was cooler with a $T_{\rm eff}$ of 3525 K being derived. For V11, we also checked the $T_{\rm eff}$ with the line depth ratio (LDR) method, based on the relation between LDR and temperature (Taniguchi *et al.* 2018). We found that the two $T_{\rm eff}$ values, one from color-temperature calibration and one from LDR, were consistent.

The surface gravity ($\log g$) was determined based on the $T_{\rm eff}$, Ks magnitude and distance modulus. Assuming a mass of $0.6\,M_{\odot}$, $\log g \sim 0.0$ was derived for all the three stars. Their microturbulences were set to be $V_{\rm t} = 2.0\,km\,s^{-1}$, following the prescriptions from literature for this kind of cool giant stars (e.g. Origlia *et al.* 2013).

4. Chemical Abundance Analysis

After carefully checking the lines covered by the spectra, the lines of eight elements, i.e. Na, Mg, Si, S, Ca, Fe, Ti and Sr, can be identified clearly in the spectra. Considering Miras are cooler so that molecular lines are stronger in their spectra, we further filtered our line list to avoid probable contamination from molecular lines. Then we measured elemental abundances through spectral synthesis using MOOG (Sneden 1973, 2017 version), adopting the MARCS model atmospheres (Gustafsson *et al.* 2008). Figure 3 shows a spectral window comparing synthetic and observed spectra, where the key lines are also indicated.

The detailed abundance determination was firstly carried out for V11, taking advantage of the best quality of its spectrum among the three sample stars. We derived the

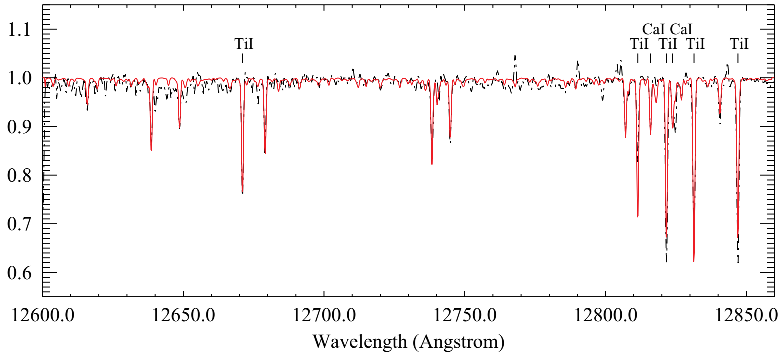

Figure 3. An example of the synthesized spectrum (red line) compared with the observed one (black dash-dotted line). Some key lines are marked.

preliminary abundances of iron [Fe/H] = -1.01 dex (σ = 0.21 dex) and titanium [Ti/Fe] = 0.50 dex (σ = 0.26 dex). However, the iron value is about 0.2 dex lower then the general metallicity determined from optical spectra. A similar case is also found for Arcturus which is often taken as a reference. Currently the analysis is still going on, and we will further check whether the deviation comes from a systematic difference between NIR and optical spectra, and more results are coming soon.

References

Alonso, A., Arribas, S., & Martínez-Roger, C. 1999, *A&AS*, 140, 261

Bono, G., Stetson, P. B., Sanna, N., Piersimoni, A., Freyhammer, L. M., Bouzid, Y., Buonanno, R., Calamida, A., Caputo, F., Corsi, C. E., Di Cecco, A., Dall'Ora, M., Ferraro, I., Iannicola, G., Monelli, M., Nonino, M., Pulone, L., Sterken, C., Storm, J., Tuvikene, T., & Walker, A. R. 2008, *ApJ*, 686, L87

Cardelli, Jason A., Clayton, Geoffrey C., & Mathis, John S. 1989, *ApJ*, 345, 245

Gullikson, K., Dodson-Robinson, S., & Kraus, A. 2014, *AJ*, 148, 53

Gustafsson, B., Edvardsson, B., Eriksson, K., Jørgensen, U. G., Nordlund, Å., & Plez, B. 2008, *A&A*, 486, 951

Kochanek, C. S., Shappee, B. J., Stanek, K. Z., Holoien, T. W.-S., Thompson, Todd A., Prieto, J. L., Dong, Subo, Shields, J. V., Will, D., Britt, C., Perzanowski, D., & Pojmański, G. 2017, *PASP*, 129, 4502

Lebzelter, T., Wood, P. R., Hinkle, K. H., Joyce, R. R., & Fekel, F. C. 2005, *A&A*, 432, 207

Lebzelter, T., Nowotny, W., Hinkle, K. H., Höfner, S., & Aringer B. 2014, *A&A*, 567, A143

Origlia, L., Oliva, E., Maiolino, R., Mucciarelli, A., Baffa, C., Biliotti, V., Bruno, P., Falcini, G., Gavriousev, V., Ghinassi, F., Giani, E., Gonzalez, M., Leone, F., Lodi, M., Massi, F., Montegriffo, P., Mochi, I., Pedani, M., Rossetti, E., Scuderi, S., Sozzi, M., & Tozzi, A. 2013, *A&A*, 560, A46

Sneden, Christopher Alan. 1973, *PhDT*, 180

Taniguchi, D., Matsunaga, N., Kobayashi, N., Fukue, K., Hamano, S., Ikeda, Y., Kawakita, H., Kondo, S., Sameshima, H., & Yasui, C. 2018, *MNRAS*, 473, 4993

Shappee, B. J., Prieto, J. L., Grupe, D., Kochanek, C. S., Stanek, K. Z., De Rosa, G., Mathur, S., Zu, Y., Peterson, B. M., Pogge, R. W., Komossa, S., Im, M., Jencson, J., Holoien, T. W.-S., Basu, U., Beacom, J. F., Szczygieł, D. M., Brimacombe, J., Adams, S., Campillay, A., *et al.* 2014, *ApJ*, 788, 48